Reactive electro-erosion of metals under pulse electric discharge

M. SOKOŁOWSKI, A. SOKOŁOWSKA, A. RUSEK, A. MICHALSKI, J. GLIJER
Institute of Materials Science, Warsaw Technical University, Warsaw 02-524 ul. Narbutta 85, Poland

Electro-erosion of metals (Al, Ti) was investigated from the point of view of the influence which a chemical reaction might exert on this process. Very strong "reactive electro-erosion" manifests itself in the presence of gases which can form stable compounds with electrode materials.

1. Introduction

Electro-erosion of metals occurs as a result of electric discharges between the metals, especially in the case of pulse discharges. An electric discharge process may be characterized by voltage and current time variations in the inter-electrode space.

Pulse discharge being a discharge supplied from a source of limited energy reserve, always includes the streamer phase and intermediate phase. The duration of the arc discharge phase depends both on the amount of energy stored in the supplying source and on electric parameters of the discharge circuit. Because of this, four mechanisms of turning the electrode material into the plasma state which is the electro-erosion nature, may be distinguished: evaporation [1–9], ablation [9–14], cathode sputtering [15], and mechanical disruption of metal [16–18].

In experimental investigations as well as in theoretical considerations on electro-erosion, phenomena are usually analysed taking place in vacuum or in a gas whose chemical activity is neglected. Only a few works have been concerned with electro-erosion in reactive gases, but they were interested solely in the surface condition of the electrode [19]. The aim of the present work was to investigate reactive electro-erosion of metals, i.e. a process taking place on the electrodes under pulse discharge in the atmosphere of a gas which can enter into stable chemical compounds with the metal under investigation. Moreover, the experimental methods employed in the present work also include, besides generally used measurements of the mass loss and morphological changes, observations of internal changes inside the material investigated. The results of the present investigation may be used as a basis in selecting a suitable material for the electrodes or in choosing an appropriate gas, and they may contribute to the development of electro-erosion theory.

TABLE I

Material	Mechanical properties			Thermal properties			
	Critical stress (MPa)	Young's modulus (10^4 MPa)	Poisson's ratio	Coeff. of thermal conductivity (10^3 kW m^{-1} °C^{-1})	Boiling temp. (°C)	Thermal coefficient of linear expansion (10^6 deg^{-1})	Stress due to temperature gradient $T_{melt} - T_{373\,K}$ (MPa)
Aluminium	4.9	7.05	0.34	0.22	658	24.9	1362
Duralumin	98	7.35	0.38	0.12 – 0.18	620	23.4	
Titanium	78.4	11.56	0.34	0.22	1668	8.5	2175

2. Experiments

2.1. Materials

The experimental metals were chosen so that they create stable high melting compounds with the selected gases yet differing from each other in thermal and mechanical properties which can determine the electro-erosion rate. Aluminium, duralumin and titanium were selected. Table I shows thermal and mechanical characteristics of these metals. As can be seen, Al differs essentially from duralumin only in critical stress while Ti may be distinguished from the others by its Young's modulus and thermal characteristics (especially boiling point).

The materials used in the present investigation were Al 5N, commercially pure Ti, and commercial duralumin AlMg6.

As experimental gases, spectrally pure O_2, N_2,

TABLE II

Gas	Al		Ti		Coefficient of thermal conductivity (10^{-4} kW m^{-1} °C^{-1})
	Reaction product	Melting point (° C)	Reaction product	Melting point (° C)	
O_2	Al_2O_3	2051	TiO_2	1640 decomposition	0.31
			TiO	1750	
			TiO_3	2130 decomposition	
N_2	AlN	2200–2500 decomposition	TiN	3200	0.29
H_2	AlH_3	100 decomposition	TiH_2	640	1.98
Ar	–	–	–	–	0.18
CH_4	Al_4C_3	2200 in vacuum sublimate	TiC	3067	0.37

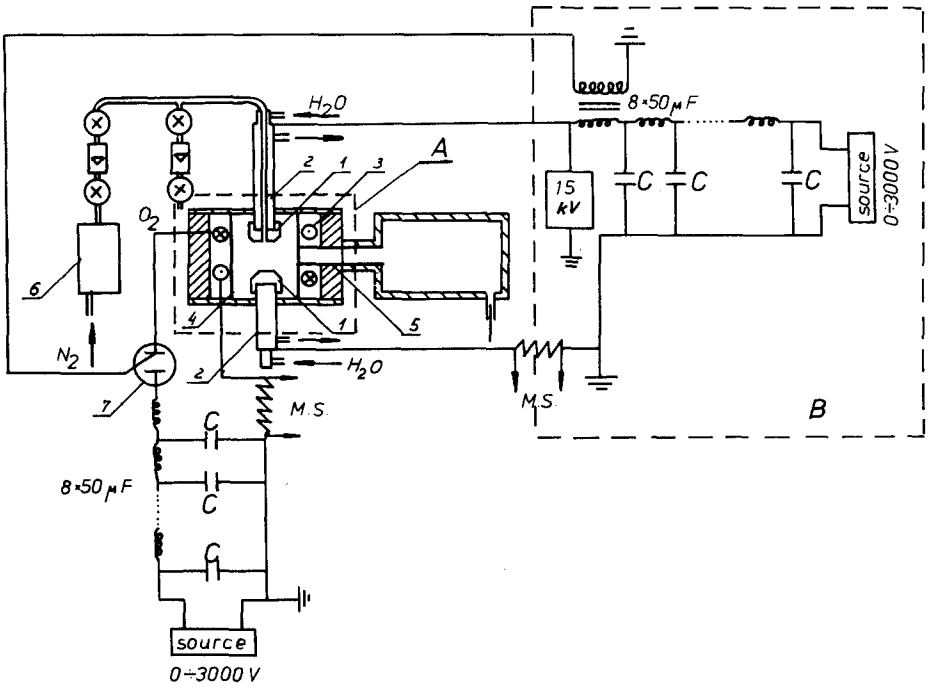

Figure 1 Schematic diagram of the experimental apparatus; 1, electrode ending cap; 2, electrodes cooled with water; 3, solenoid encapsulated in a composite material; 4, alundum chamber; 5, alundum outlet channel; 6, gas purifier; 7, trigger switch. A, T-type plasma generator, B, electric discharge circuit of T-type plasma generator.

H_2, CH_4 and Ar were used. Table II presents some properties of their compounds with the selected metals, as well as their thermal conductivity.

2.2. Experimental apparatus

The discharge was produced in a T-type plasma generator (Fig. 1). The discharge parameters are listed in Table III. The plasma produced during the inter-electrode discharge was compressed by means of a pulse magnetic field. Fig. 2 shows a discharge current oscillogram. Plasma obtained in a T-type generator was in the L.T.E. state for energies higher than 100 J and its average temperature was 10^4 K as determined by the two spectral lines density method and the continuous spectrum distribution method.

TABLE III

Pulse duration (10^{-3} sec)	Pulse repetition frequency (Hz)	Peak interelectrode voltage (V)
0.64	1	1600

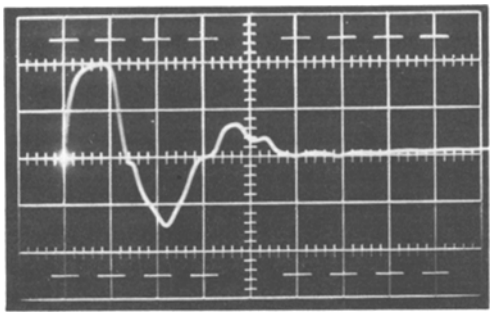

Figure 2 Current–time characteristic of the impulse discharge in the plasmatron: x-axis 0.2 msec/div; y-axis, 3.5 kA/div. Discharge voltage between the electrodes is 2000 V; discharge voltage at the magnetic field solenoid terminals is 2000 V.

2.3. Experimental methods

Each experiment lasted for 2 h (7200 discharge pulses). The results presented are the average values taken from 6 to 10 experiments.

The mass loss was measured gravimetrically with a type TA13 balance, to an accuracy of 10^{-7} kg. For metallographic observations of the electrode surfaces and their cross-sectional areas, a Neophot-Zeiss microscope was used, while the microhardness was measured using a Haneman tester at a fixed load of 100 g.

Dislocation microstructures of the electrodes as well as forms of electro-erosion products were observed with the use of a BM 300 Philips transmission electron microscope. Phase analysis of the electrodes and electro-erosion products was performed using an X-ray Philips diffractometer.

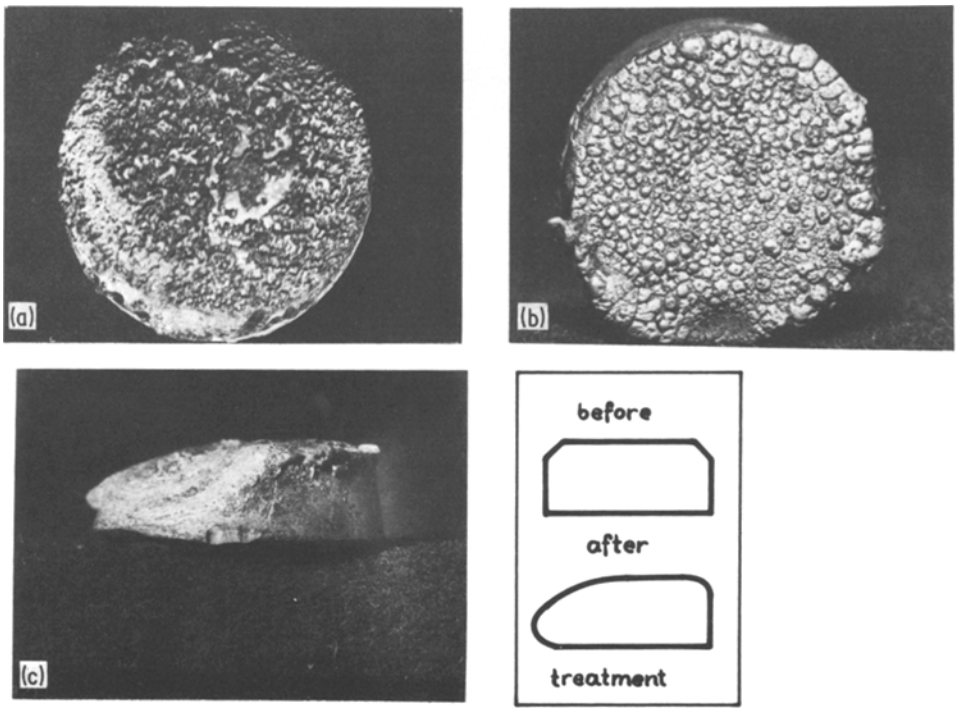

Figure 3 Typical changes in the electrode endings. (a) Front surface of Al electrode treated in O_2, (b) front surface of Ti electrode treated in N_2, (c) side view of the electrode ending cap.

For discharge plasma spectrum analysis an ISP22 spectrograph was used.

3. Results

Under the influence of discharges the shape of the electrode endings was undergoing typical changes (Fig. 3a to c). Distortion of the electrode material was observed, indicative of squeezing the metal in the direction of the plasma outlet. The face surface was covered with bulges and craters giving evidence of material melting, which was particularly noticeable for Al electrodes. In the case of a Ti electrode treated in N_2, the electrode surface was additionally coated with a golden film (TiN).

In all cases of electro-erosion carried out in a reactive gas, a highly dispersed aerosol was obtained composed of a metal compound with the gas. Specificity of the aerosol and its generation were described in our previous work [20]. The shape and size of the aerosol particles (Fig. 4a to c) indicate that they are crystallized from the plasma rather than are products of a film stripped away from the elctrode surface. When inactive gases were used, the particles of electrode metal obtained had the form of relatively large polycrystalline spherules of 1 μm diameter.

The erosion rate, i.e. a mass loss per coulomb, was evidently different for discharges taking place in a reactive gas as compared to an inactive gas. In all cases, electro-erosion performed in a reactive gas atmosphere was much larger than in an inactive gas (Table IV). As can be seen, electro-erosion of Al in N_2 and O_2 is by two orders of magnitude greater than in Ar, the kind of the reactive gas (N_2 or O_2) employed being of no significant importance. It should be noted that the results obtained in H_2, although AlH_3 is an unstable volatile compound, also show to some extent an increased electro-erosion rate.

TABLE IV

Metal	Gas	Electro-erosion rate (10^6 kg C^{-1})	Electro-erosion rate in respect to Ar
Al	O_2	0.350	80.61
Al	N_2	0.320	70.82
Al	H_2	0.090	2.52
Al	Ar	0.025	–
Duralumin	O_2	0.390	–
Ti	N_2	0.010	1.15
Ti	CH_4	0.182	20.1
Ti	Ar	0.005	–

It was further found that in a reactive gas, the higher the energy dissipated in a pulse, the higher the erosion rate, while in an inactive gas the erosion rate was found to be unaffected by the discharge energy (Fig. 5). The influence of a gas flow velocity on the increase of the mass loss of the electrode is also much stronger for a reactive gas than for an inactive gas (Fig. 6).

The structure of metals exposed to electric pulse discharges was undergoing some changes dependent both on the kind of metal and the gas employed. In the case of Al, the structure of the material beneath the face became fine grained (see Fig. 7a). The grain diameter decreased from about 10^{-3} m to about 10^{-5} m and the metal layer of refined structure was 20×10^{-5} m thick. When Al is subject to pulse discharges in O_2 or N_2 the refinement of structure is not so significant as in H_2 and the depth of the transformed layer amounts only to about 16×10^{-5} m. It is probable that this is connected with a high thermal conductivity of H_2. The refined grains are now elongated

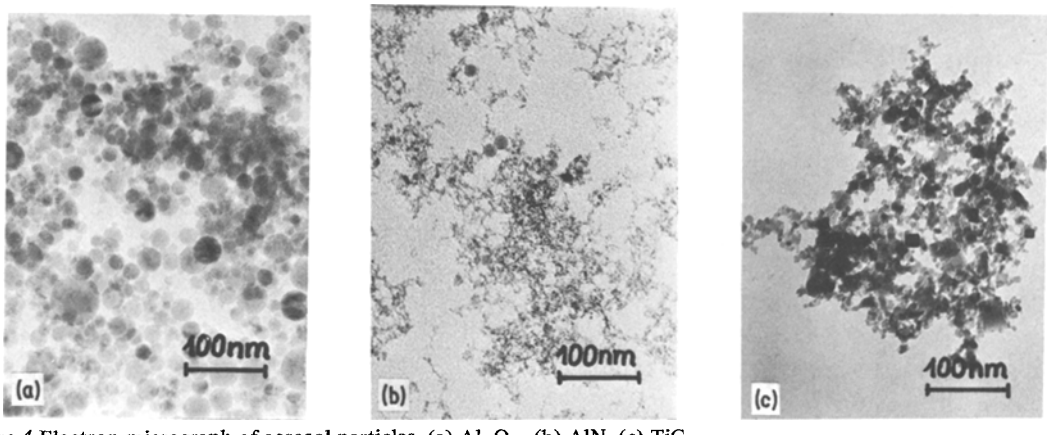

Figure 4 Electron micrograph of aerosol particles. (a) Al_2O_3, (b) AlN, (c) TiC.

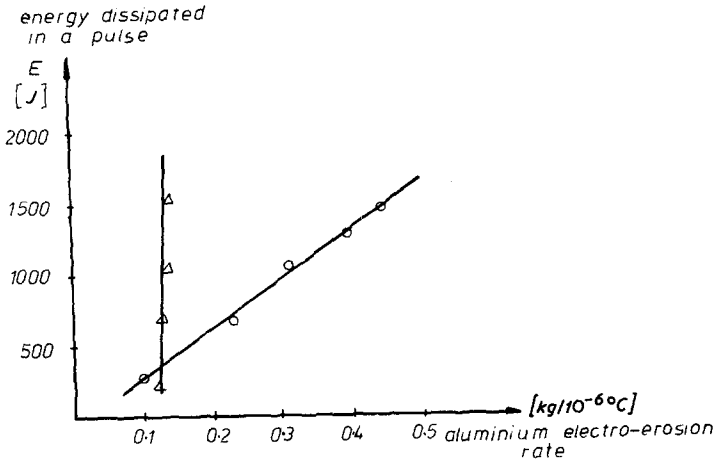

Figure 5 Electro-erosion rate for aluminium depending on energy dissipated in a pulse. ○ O_2 — 0.1 m^3 sec^{-1}; + Ar — 2 m^3 sec^{-1}; △ H_2 — 30 m^3 sec^{-1}

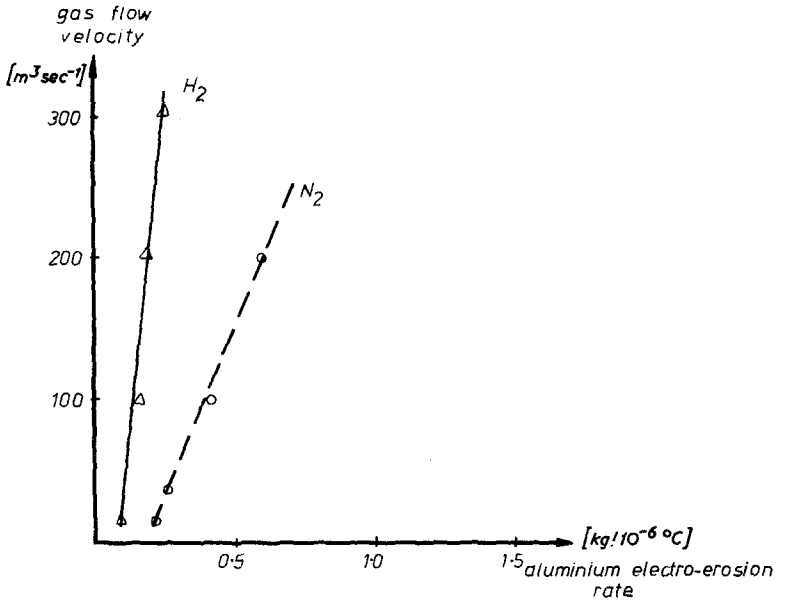

Figure 6 Electro-erosion rate for aluminium on gas flow velocity. Energy dissipated in a pulse 512 J. ○ N_2, △ H_2.

in the direction perpendicular, or in some cases parallel, to the front surface. Slip lines can be observed generally running parallel to the surface but partially whirled. Also in the zone close to the surface some dislocation centres can be found (Fig. 7b), and electron microscope observations show the presence of sub-boundaries in the grains (Fig. 7c).

All these changes observed in Al represent a typical image of a material which had been exposed to variation of stress and temperature with time and space.

In order to compare similar materials differing in their critical stress values, investigations on duralumin were performed showing quite good similarity in behaviour between the two metals. The erosion rate for duralumin treated in O_2 was found to be the same as for Al; however, the symptoms of plastic deformation observed in duralumin were less significant than for Al (Fig. 8).

Investigations on Ti were carried out to compare materials having different boiling points. Important differences were found in the behaviour of Ti compared with Al. Although the erosion rate for Ti treated in N_2, which functions as a reactive gas for Ti, was higher than in any inactive gas, it was not as high as in Al. The erosion rate for Ti was found to be dependent on the kind of reactive gas employed in the process. The highest erosion rate was measured in the presence of CH_4. These

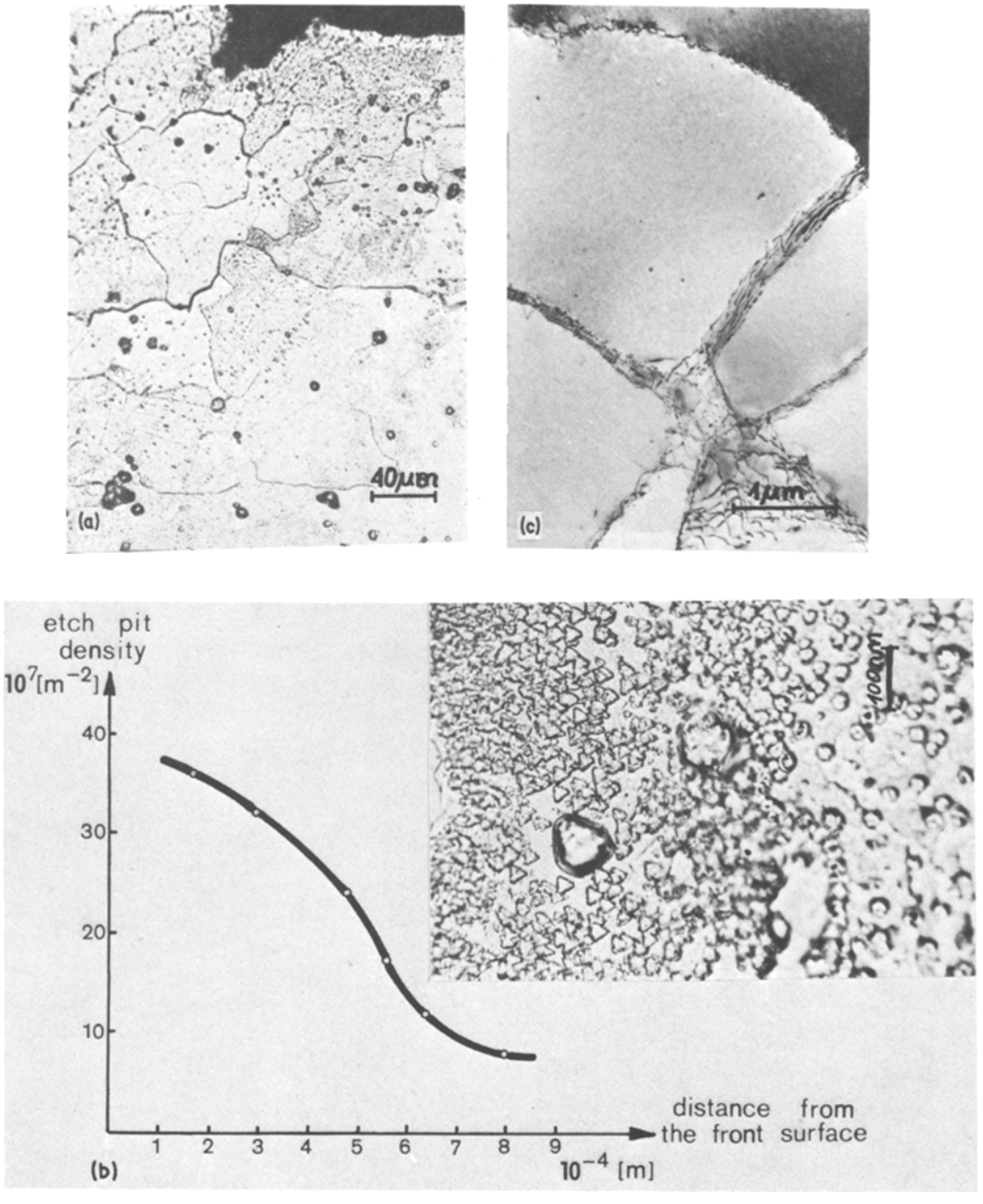

Figure 7 Influence of the impulse discharge in O_2 on Al structure. (a) Sub-surface grain refinement; etching T46HF + $46H_2O$ + 8HCl. (b) Etch pit density depending on a distance from the front surface; (c) grain sub-boundaries in sub-surface.

dependences are given in Table IV.

Metallographic observations of the cross-sections of the Ti electrode endings revealed reactive diffusion of the gas into the metal. On the Ti surface exposed to pulse discharges in N_2, a thick TiN film is produced, as shown in Fig. 9a. Reactive diffusion of C taking place in the Ti electrode treated in CH_4 results in a thick compound or diffusion layer with fine TiC dispersives, as can be seen in Fig. 9b. It can be assumed that these phenomena are connected with a good solubility of N_2 and C in Ti. For comparison, a cross-section

Figure 8 Plastic deformation in duralumin; etching T46HF + 46H_2O + 8HCl.

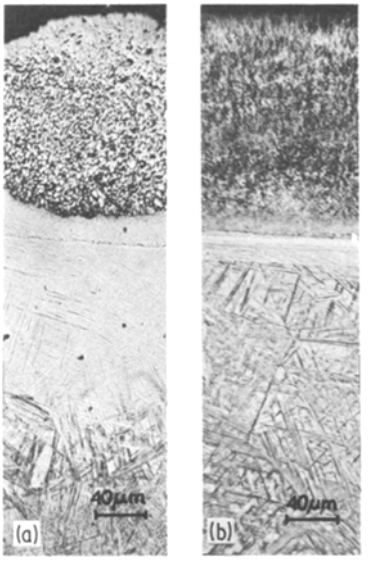

Figure 9 Reactive diffusion of gas atoms taking place in Ti electrodes. (a) Ti treated in N_2; (b) Ti treated in CH_4, etching TMi37Ti.

Figure 10 Ti electrode treated in Ar; etching TMi 37Ti.

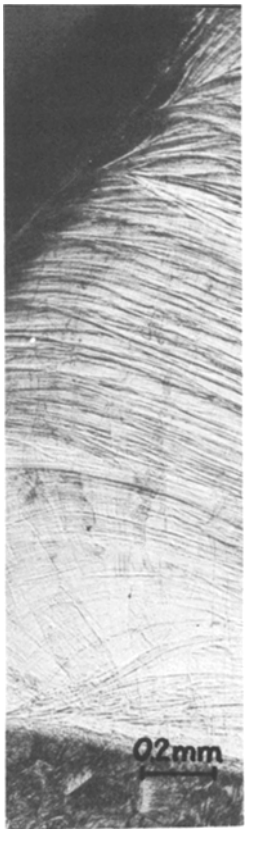

Figure 11 Plastic deformation in titanium; etching TMi37Ti.

of Ti electrode ending treated in Ar is shown in Fig. 10.

In all microphotographs shown here, an α' Ti layer, resistant to etching, is apparent which being indicative of a phase transformation of Ti, constitutes a sort of temperature marker. In the area where this layer is present, the temperature had to be higher or equal to the transformation temperature which is 882.5° C.

In many cases metallographic investigations show no effect of plastic deformation in Ti. However, under certain conditions (long process duration, great discharge frequency, etc.) which could elevate the temperature, plastic deformation was observed (Fig. 11).

4. Conclusions

On the basis of the results presented above some general statements may be proposed, differentiating electro-erosion of a metal, which was placed in a gas entering into stable chemical compounds with the metal, as a specific process essentially different from electro-erosion under vacuum or inactive gas conditions. By way of analogy to other known terms, e.g. chemical corrosion, the process described here may be termed reactive electro-erosion.

(1) The most general feature of the reactive electro-erosion seems to be the fact that a highly-dispersed aerosol is obtained as a reaction product. The generation of the highly dispersed aerosol does not depend on either mechanical and thermal properties of the metal or on electric discharge parameters, which can be taken as evidence that the method of turning the electrode material into the plasma state is of no importance for this process.

(2) The character of the reactive electro-erosion process depends on the kind of metal employed. When Al and duralumin are used, chemical activity of the N_2 and O_2 affects the erosion rate to such an extent that the influence of other factors known from the literature cannot be observed, e.g. the electrode shape (the effect of an electric field intensity), mechanical properties of the metal which determine some processes connected with thermo-mechanical fatigue of the material, etc. Furthermore, it was observed that the reactive electro-erosion rate increases when the gas flow velocity is increasing. The only possible explanation for these facts is that under the conditions of our experiments erosion of Al and duralumin was essentially due to evaporation which, as may be supposed, is intensified here by removal of metal vapours from above the electrode surface throughout the chemical reaction in the plasma. It is symptomatic that in this case the changes observed in the material structure are typically bound with the variation of stress and temperature gradients with time, the changes most probably resulting from thermal stresses rather than caused by ablation.

(3) In the case of Ti, which has a high boiling point and good solubility of reactive gases, the influence of chemical activity of the gas is manifested in quite a different way. The main role is allotted to chemical reaction with the electrode material and not with its vapour. The increase in the erosion rate in a reactive gas is much less than for Al and duralumin. It may be assumed that under the conditions of our experiments evaporation is not the main mechanism of electro-erosion in Ti.

Acknowledgements

This work was supported by the Ministry of Science, Higher Education and Technology under contract MR.I.21.

References

1. M. P. REECE, *Proc. Inst. Elec. Eng.* **119** (1963) 793.
2. W. D. DAVIS and H. C. MILLER, *J. Appl. Phys.* **40** (1969) 2212.
3. A. E. GUILE and A. H. HITCHOCK, *J. Phys. D. Appl. Phys.* 7 (1974) 597.
4. J. D. COBINE and G. A. FARRALL, *J. Appl. Phys.* **31** (1960) 2296.
5. A. A. PLJUTO, V. N. RYZKOW and A. T. KASIM, *Z.E.T.F.* 47 (1964) 434.
6. J. D. COBINE and E. G. BURGER, *J. Appl. Phys.* **26** (1955) 895.
7. K. SCHONBACH, *Z. angew. Phys.* 32 (1971) 253.
8. S. J. BRAGIŃSKI, *Z.E.T.F.* 34 (1958) 1459.
9. N. W. AFANASIEW, S. N. KAPELJAN and L. P. FILIPPOW, "Chimija i fizika niskotemperaturnoj plazmy" Trudy I Międzyn. Konf. po chimii i fizikie niskotemperaturnoj plazmy J.M.U. (1971) p. 106.
10. M. A. SUŁTANOW and P. R. KISIELEWSKIJ, *Tieplofizika Wysokich Temperatur* 4 (1966) 375.
11. B. A. AGEEW and M. A. SUŁTANOW, *ibid* **11** (1973) 498.
12. M. A. SUŁTANOW, *ibid* 8 (1970) 963.
13. K. DIMOFF and A. K. WIJH, J.E.E.E. Conference record-abstracts. The Second International Conference On Plasma Science, Ann Arbor, Michigan, USA (1975).
14. K. DIMOFF, W. SOUILHAL and B. SARAH The Fourth International Conference on Gas Discharges, London (1976).
15. F. LLEWELLYN JONES, *Nature* **157** (1946) 299.

16. N. B. ZOŁOTYCH, "Fizichzeskije osnowy elektroiskrowej obrabotki mietałłow" (G.S.T.T.L., Moskwa, 1953).
17. K. ALBINSKI, "Elektroerozyjna obróbka metali" (PWT, Warszawa, 1954).
18. Z. POLAŃSKI, "Elektroiskrowe drażenie metali erodami kompensacyjnymi" (NT, Warszawa, 1965).
19. A. E. GUILE and A. M. HITCHOCK, *J. Phys. D. Appl. Phys.* 8 (1975) 427.
20. M. SOKOŁOWSKI, A. SOKOŁOWSKA, M. MICHALSKI, B. GOKIELI, R. ROMANOWSKI and A. RUSEK, *J. Cryst. Growth* 42 (1977) 507.
21. G. W. McCLURE, *J. Appl. Phys.* 45 (1974) 2078.
Received 11 April and accepted 18 September 1978.